

Symmetry controlled photo-selection and charge separation in butadiyne-bridged donor-bridge-acceptor compounds

Xiao Li,^a Jesús Valdiviezo,^b Susannah D. Banziger,^e Peng Zhang,^b Tong Ren,^{e*} David N. Beratan,^{b,c,d*} and Igor V. Rubtsov^{a*}

^a Department of Chemistry, Tulane University, New Orleans, LA 70118, USA

^b Department of Chemistry, Duke University, Durham, North Carolina 27708, USA

^c Department of Physics, Duke University, Durham, North Carolina 27708, USA

^d Department of Biochemistry, Duke University, Durham, North Carolina 27710, USA

^e Department of Chemistry, Purdue University, West Lafayette, Indiana 47907, USA

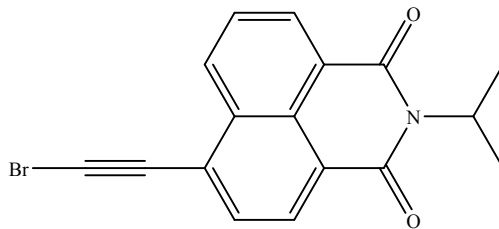
Table of Contents

1. Details of synthesis
2. Normal mode frequencies DFT computed for Si-C4-NAP, Ph-C4-NAP, and D-C4-NAP (Tables S1-S5).
3. DFT computed frontier orbital compositions for D-C4-NAP and Si-C4-NAP (Figures S1-S2, S9-S10).
4. TR-IR spectra and kinetic traces for Si-C4-NAP in toluene (Figures S3-S8)
5. ¹H NMR and ¹³C NMR spectra (Figures S11-S17)

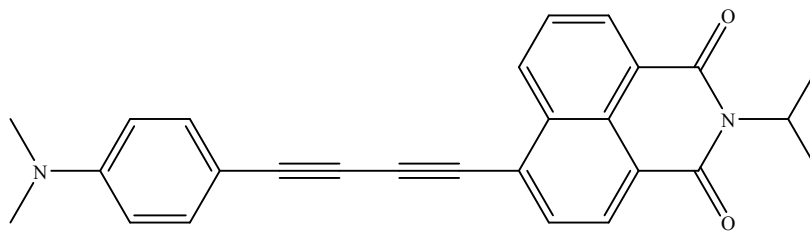
1. Details of Synthesis

1.1 Materials and measurements

4-ethynyl-*N*-isopropyl-1,8-naphthalimide (**NAP^{iPr}C₂H**) was prepared according to literature procedure¹. THF was distilled over Na/benzophenone under a N₂ atmosphere. CH₂Cl₂ was distilled over CaH₂ under N₂. *N,N*-Dimethyl-4-[(trimethylsilyl)ethynyl]aniline was purchased from Sigma Aldrich, triethylsilylacetylene was purchased from Oakwood Chemical, and pyridine was purchased from Mallinckrodt Chemicals and dried over hot sieves. The synthesis of 4-bromo-ethynyl-*N*-isopropyl-1,8-naphthalimide (**BrC₂NAP^{iPr}**) was performed under ambient atmosphere. All other reactions were carried out using Schlenk techniques under N₂. UV-Vis-NIR spectra were obtained with a JASCO V-670 UV-Vis-NIR spectrophotometer. Infrared spectra were obtained on a JASCO FT-IR 6300 spectrometer via ATR on a ZnSe crystal. Emission spectra were measured on a Varian Cary Eclipse fluorescence spectrophotometer and quantum yields were measured on Edinburgh Instruments FLS980 steady state fluorescence spectrometer using an integrating sphere attachment. ¹H NMR spectra were recorded on a Varian MERCURY300 NMR and a Varian Inova 300.

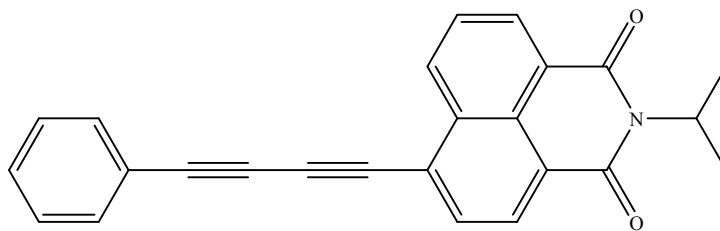


Preparation of 4-bromo-ethynyl-*N*-isopropyl-1,8-naphthalimide (BrC₂NAP^{iPr}). 4-Ethynyl-*N*-isopropyl-1,8-naphthalimide (800 mg, 3.0 mmol) was dissolved in acetone with *N*-bromosuccinimide (1.08 grams, 6.1 mmol) and AgNO₃ (52 mg, 0.31 mmol). The solution was stirred at room temperature overnight. The crude reaction mixture was purified via a silica plug (1:1 Hexanes:CH₂Cl₂) to yield 980 mg of the desired product as a light yellow solid (94% based on 4-ethynyl-*N*-isopropyl-1,8-naphthalimide). ¹H NMR (300 MHz, Chloroform-*d*) δ 8.63 – 8.56 (m, 2H), 8.50 (d, *J* = 7.6 Hz, 1H), 7.88 (d, *J* = 7.4 Hz, 1H), 7.82 (dd, *J* = 8.4, 7.1 Hz, 1H), 5.46 – 5.39 (m, 1H), 1.59 (d, *J* = 7.0 Hz, 6H). Visible spectra, λ_{max} (nm, ε (M⁻¹ cm⁻¹)): 350 (34,400), 367 (31,300); IR (cm⁻¹): C=O: 1653 (s), 1693 (s); C≡C: 2188 (s).

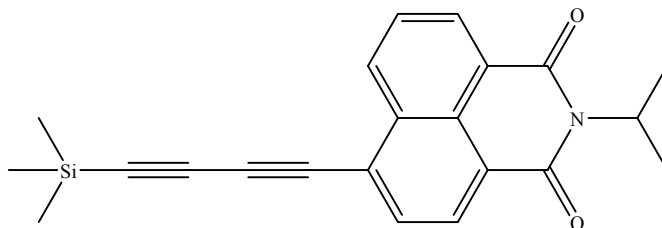


Preparation of D-C₄-NAP^{iPr}. A 3-neck round bottom flask was fitted with a side-arm containing CuI (190 mg, 1.0 mmol) and charged with 4-ethynyl-*N,N*-dimethylaniline (290 mg, 2.0 mmol) and dry THF (10 mL). Upon cooling to -10°C, *n*BuLi (1.6 M in hexane, 1.25 mL, 2.0 mmol) was added while stirring and warming to 0°C. After 20 min, CuI was added and the

solution immediately turned bright yellow. It was allowed to stir and warm to room temperature for 1 hr. Pyridine (29 mL) was added while the solution stirred at -10°C . A solution of dry THF (15 mL) and $\text{BrC}_2\text{NAP}^{\text{iPr}}$ (340 mg, 1.0 mmol) was added dropwise over 1 h, the solution turned steadily more red. Upon complete addition, the reaction was allowed to stir an additional 10 min and quenched with CH_3OH . The solvent was removed under vacuum. The crude material was extracted from brine with CH_2Cl_2 and dried over MgSO_4 . Purification of the vibrant red solution was achieved through column chromatography (silica gel, 1:1 Hexane: CH_2Cl_2) yielded 205 mg of **D-C₄-NAP^{iPr}** as a bright red solid. (51% based on $\text{BrC}_2\text{NAP}^{\text{iPr}}$). ^1H NMR (300 MHz, Chloroform-*d*) δ 8.65 (d, $J = 8.3$ Hz, 1H), 8.59 (d, $J = 7.3$ Hz, 1H), 8.48 (d, $J = 7.6$ Hz, 1H), 7.90 (d, $J = 7.7$ Hz, 1H), 7.80 (t, $J = 7.8$ Hz, 1H), 7.46 (d, $J = 8.7$ Hz, 2H), 6.64 (d, $J = 8.8$ Hz, 2H), 5.42 (hept, $J = 6.7$ Hz, 1H), 3.03 (s, 6H), 1.60 (d, $J = 6.9$ Hz, 6H). ^{13}C NMR (75 MHz, CDCl_3) δ 164.09, 163.79, 150.76, 133.99, 132.06, 131.99, 131.58, 131.39, 129.96, 127.91, 127.50, 126.49, 123.44, 122.66, 111.57, 106.86, 87.85, 84.22, 77.68, 77.46, 77.04, 76.62, 72.11, 45.41, 40.16, 19.90. Visible spectra, λ_{max} (nm, ϵ ($\text{M}^{-1} \text{cm}^{-1}$)): 337 (26,000), 454 (18,200); IR (cm^{-1}): C=O: 1653 (s), 1692 (s); C \equiv C: 2118 (w), 2133 (m), 2184 (s).



Preparation of Ph-C₄-NAP^{iPr}. A 3-neck round bottom flask was fitted with a side-arm containing CuI (280 mg, 1.5 mmol) and charged with phenylacetylene (0.5 mL, 4.6 mmol) and dry THF (5 mL). Upon cooling to -10°C , $n\text{BuLi}$ (1.6 M in hexane, 1.6 mL, 2.6 mmol) was added while stirring and warming to 0°C . After 20 min, CuI was added and the solution immediately turned orange. It was allowed to stir and warm to room temperature for 1 hr. Pyridine (15 mL) was added while the solution stirred at -10°C . A solution of dry THF (20 mL) and $\text{BrC}_2\text{NAP}^{\text{iPr}}$ (430 mg, 1.2 mmol) was added dropwise over 1.5 h, the solution turned red. Upon complete addition, the reaction was allowed to stir an additional 10 min and quenched with CH_3OH . The solvent was removed under vacuum. The crude material was extracted from brine with CH_2Cl_2 and dried over MgSO_4 . Purification was achieved through column chromatography (silica gel, 1:1 Hexane: CH_2Cl_2). Recrystallization from CH_2Cl_2 with hexane yielded 189 mg of **Ph-C₄-NAP^{iPr}** as a yellow solid. (42% based on $\text{BrC}_2\text{NAP}^{\text{iPr}}$). ^1H NMR (300 MHz, Chloroform-*d*) δ 8.66 – 8.58 (m, 2H), 8.50 (d, $J = 7.6$ Hz, 1H), 7.94 (d, $J = 7.6$ Hz, 1H), 7.82 (t, $J = 7.8$ Hz, 1H), 7.58 (dd, $J = 7.7, 1.5$ Hz, 2H), 7.46 – 7.34 (m, 3H), 5.42 (hept, $J = 6.8$ Hz, 1H), 1.60 (d, $J = 6.9$ Hz, 6H). ^{13}C NMR (75 MHz, CDCl_3) δ 163.98, 163.69, 132.55, 132.08, 132.07, 131.76, 131.49, 129.87, 129.75, 128.51, 127.86, 127.73, 125.64, 123.51, 123.26, 121.05, 85.26, 82.82, 78.06, 77.46, 77.04, 76.62, 73.47, 45.48, 19.88. Visible spectra, λ_{max} (nm, ϵ ($\text{M}^{-1} \text{cm}^{-1}$)): 382 (31,700), 396 (31,700); IR (cm^{-1}): C=O: 1655 (s), 1693 (s); C=C: 2143 (m), 2146 (m), 2210 (s).



Preparation of Me₃Si-C₄-NAP^{iPr}. A 3-neck round bottom flask was fitted with a side-arm containing CuI (450 mg, 2.4 mmol) and charged with trimethylsilyl acetylene (1.5 mL, 10.6 mmol) and dry THF (10 mL). Upon cooling to -10°C, nBuLi (2.5 M in hexane, 4.0 mL, 9.6 mmol) was added while stirring and warming to 0°C. After 20 min, CuI was added and the solution immediately turned orange. It was allowed to stir and warm to room temperature for 1 hr. Pyridine (20 mL) was added while the solution stirred at -10°C. A solution of dry THF (30 mL) and BrC₂NAP^{iPr} (1.0 gram, 2.9 mmol) was added dropwise over 1.5 h, the solution turned darker red. Upon complete addition, the reaction was allowed to stir an additional 10 min and quenched with CH₃OH. The solvent was removed under vacuum. The crude material was extracted from brine with CH₂Cl₂ and dried over MgSO₄. Purification was achieved by rinsing the red solution through a CH₂Cl₂ silica plug followed by column chromatography (silica gel, CH₂Cl₂). Recrystallization from CH₂Cl₂ with CH₃OH yielded 490 mg of Me₃Si-C₄-NAP^{iPr} as a yellow solid. (47% based on BrC₂NAP^{iPr}). ¹H NMR (300 MHz, Chloroform-*d*) δ 8.62 – 8.60 (m, 1H), 8.58 (d, *J* = 2.7 Hz, 1H), 8.48 (d, *J* = 7.6 Hz, 1H), 7.91 (d, *J* = 7.6 Hz, 1H), 7.81 (dd, *J* = 8.3, 7.4 Hz, 1H), 5.41 (p, *J* = 6.9 Hz, 1H), 1.59 (d, *J* = 6.9 Hz, 6H), 0.29 (s, 9H). ¹³C NMR (75 MHz, CDCl₃) δ 163.95, 163.65, 132.36, 132.26, 131.69, 131.51, 129.80, 127.82, 127.78, 125.22, 123.53, 123.42, 95.08, 87.11, 82.81, 77.45, 77.03, 76.60, 73.15, 45.48, 19.86, 1.18. Visible spectra, λ_{max} (nm, ε (M⁻¹ cm⁻¹)): 366 (17,200), 385 (19,800); IR (cm⁻¹): C=O: 1654 (s), 1696 (s); C≡C: 2101 (s), 2205 (m).

Table S1. TD-DFT computed vibrational frequencies and IR intensities (I) for D-C4-NAP in toluene and DCM in the ground and excited states at $\theta = 0$.

States	$\nu_{C=O,as} / \text{cm}^{-1}$ ($I / \text{km/mol}$)	$\nu_{C=O,ss} / \text{cm}^{-1}$ ($I / \text{km/mol}$)	$\nu_{C=C,as} / \text{cm}^{-1}$ ($I / \text{km/mol}$)	$\nu_{C=C,ss} / \text{cm}^{-1}$ ($I / \text{km/mol}$)
In toluene				
S_0	1793.6 (594)	1831.5 (571)	2257.7 (45)	2328.4 (1602)
S_3 (TD-DFT)	1740.5 (776)	1780.1 (878)	2129.8 (514)	2197.5 (3077)
S_1 (TD-DFT)	1750.1 (825)	1784.5 (2941)	2139.2 (2387)	2187.7 (19729)
T_1 (variational)	1738.9 (671)	1789.3 (1257)	2020.5 (108)	2129.1 (3361)
In DCM				
S_0	1781.2 (812)	1823.5 (693)	2254.1 (101)	2322.3 (2152)
S_3 (TD-DFT)	1724.2 (1110)	1768.8 (1326)	2124.3 (1051)	2191.4 (4112)
S_1 (TD-DFT)	1731.2 (1309)	1771.0 (3690)	2136.1 (1744)	2188.3 (16318)
T_1 (variational)	1728.1 (1114)	1776.2 (2524)	2065.0 (3209)	2119.2 (6840)

Table S2. TD-DFT computed vibrational frequencies and IR intensities (I) for Ph-C4-NAP in toluene and DCM in the ground and excited states at $\theta = 0$.

States	$\nu_{C=O,as} / \text{cm}^{-1}$ ($I / \text{km/mol}$)	$\nu_{C=O,ss} / \text{cm}^{-1}$ ($I / \text{km/mol}$)	$\nu_{C=C,as} / \text{cm}^{-1}$ ($I / \text{km/mol}$)	$\nu_{C=C,ss} / \text{cm}^{-1}$ ($I / \text{km/mol}$)
In toluene				
S_0	1795.2 (592)	1833.7 (507)	2266.0 (0)	2349.2 (189)
S_4 (TD-DFT)	1736.9 (787)	1773.7 (2787)	2147.5 (295)	2313.0 (31540)
S_1 (TD-DFT)	1752.3 (735)	1791.6 (2063)	2120.5 (447)	2144.8 (957)
T_1 (variational)	1732.6 (513)	1794.7 (812)	1970.2 (525)	2157.8 (369)
In DCM				
S_0	1782.8 (807)	1825.5 (622)	2264.4 (1)	2347.6 (244)
S_4 (TD-DFT)	1720.8 (1234)	1761.7 (3335)	2148.3 (149)	2321.9 (33594)
S_1 (TD-DFT)	1735.7 (1067)	1778.3 (2921)	2119.1 (788)	2144.7 (375)
T_1 (variational)	1723.7 (736)	1783.4 (1156)	1971.7 (825)	2155.4 (681)

Table S3. TD-DFT computed vibrational frequencies and IR intensities (*I*) for Si-C4-NAP in toluene and DCM in the ground and excited states at $\theta = 0$.

States	$\nu_{C=O,as} / \text{cm}^{-1}$ (<i>I</i> / km/mol)	$\nu_{C=O,ss} / \text{cm}^{-1}$ (<i>I</i> / km/mol)	$\nu_{C=C,as} / \text{cm}^{-1}$ (<i>I</i> / km/mol)	$\nu_{C=C,ss} / \text{cm}^{-1}$ (<i>I</i> / km/mol)
In toluene				
S ₀	1795.7 (591)	1834.0 (456)	2224.3 (113)	2344.0 (2)
S ₁ (TD-DFT)	1745.2 (729)	1783.4 (960)	2104.2 (57)	2126.4 (0.5)
T ₁ (variational)	1731.5 (497)	1790.0 (596)	1997.7 (363)	2152.1 (15)
In DCM				
S ₀	1783.3 (805)	1826.0 (566)	2221.9 (114)	2343.1 (2)
S ₁ (TD-DFT)	1728.5 (1056)	1771.9 (1422)	2107.9 (184)	2128.8 (4)
T ₁ (variational)	1722.3 (723)	1780.7 (817)	1997.4 (519)	2150.7 (7)

Table S4. TD-DFT computed vibrational frequencies and IR intensities (*I*) for D-C4-NAP with different dihedral angles in DCM in the ground and excited states.

Dihedral angle / degrees	$\nu_{C=O,as}$ / cm^{-1} (<i>I</i> / km/mol)	$\nu_{C=O,ss}$ / cm^{-1} (<i>I</i> / km/mol)	$\nu_{C=C,as}$ / cm^{-1} (<i>I</i> / km/mol)	$\nu_{C=C,ss}$ / cm^{-1} (<i>I</i> / km/mol)
Ground state				
0	1781.2 (812)	1823.5 (693)	2254.1 (101)	2322.3 (2152)
90	1782.4 (806)	1825.0 (597)	2255.6 (105)	2339.7 (854)
Excited state S_1				
0	1731.2 (1309)	1771.0 (3690)	2136.1 (1744)	2188.3 (16317)
15	1731.5 (1322)	1771.2 (3706)	2132.1 (1865)	2177.1 (15966)
30	1732.2 (1385)	1771.8 (3711)	2119.8 (2650)	2145.3 (15044)
45	1733.1 (1500)	1772.5 (3702)	2105.1 (4275)	2094.9 (14620)
60	1734.3 (1609)	1773.4 (3667)	2081.7 (803)	2060.8 (21051)
75	1735.2 (1654)	1773.8 (3617)	2068.0 (1850)	2044.3 (22509)
90	1735.3 (1671)	1773.9 (3573)	2063.9 (2661)	2040.0 (22483)
Excited state S_2				
0	1768.7 (962)	1794.2 (944)	1814.9 (869)	2130.3 (1557)
15	1765.0 (1041)	1797.0 (1986)	1822.4 (179)	2119.5 (2379)
30	1747.0 (1140)	1784.6 (2694)	1935.0 (463)	1984.0 (1749)
45	1732.2 (1089)	1772.4 (2212)	2081.8 (3)	1963.4 (1041)
60	1727.2 (1085)	1769.7 (1744)	2146.0 (178)	2056.0 (136)
75	1725.2 (1104)	1769.1 (1432)	2180.9 (2065)	2109.2 (430)
90	1724.2 (1110)	1768.8 (1327)	2191.4 (4112)	2124.2& (1051)

Table S5. TD-DFT computed energy, dipole moment and oscillator strength at different dihedral angles for D-C4-NAP in DCM in the ground and excited states.

Dihedral angle / degrees	Energy / eV	μ / D	f
Ground state			
0	0.000	11.6	-
90	0.025	10.7	-
Excited state S ₁			
0	2.444	32.0	1.79
15	2.446	32.4	1.70
30	2.450	33.6	1.42
45	2.451	35.3	0.97
60	2.449	37.1	0.47
75	2.443	38.3	0.12
90	2.439	38.7	0.00
Excited state S ₂			
0	3.212	16.6	0.00
15	3.216	16.7	0.10
30	3.209	18.3	0.36
45	3.159	18.9	0.63
60	3.105	18.0	0.92
75	3.068	17.0	1.15
90	3.055	16.6	1.24

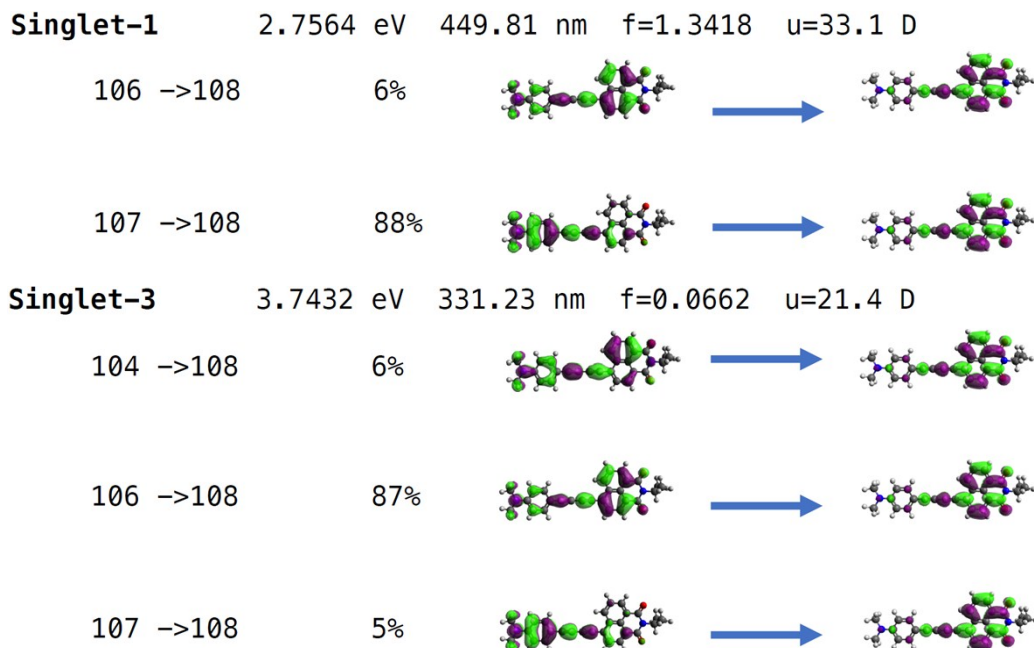


Fig. S1. TD-DFT results showing the dominant orbital contribution to the S_1 and S_3 state for D-C4-NAP in DCM. The transition energy, wavelength, oscillator strength (f) and dipole moment are shown.

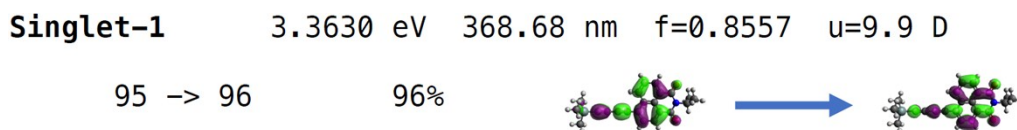


Fig. S2. TD-DFT results showing the dominant orbital contribution to the S_1 state for Si-C4-NAP in DCM. The transition energy, wavelength, oscillator strength (f) and dipole moment are shown.

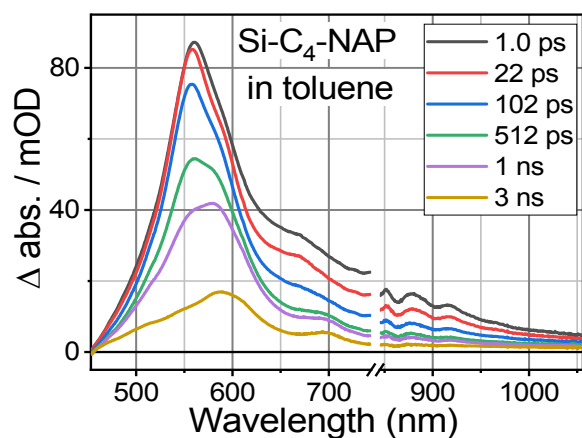


Fig. S3. Transient spectra in visible region for Si-C4-NAP in toluene excited by 400 nm pulses.

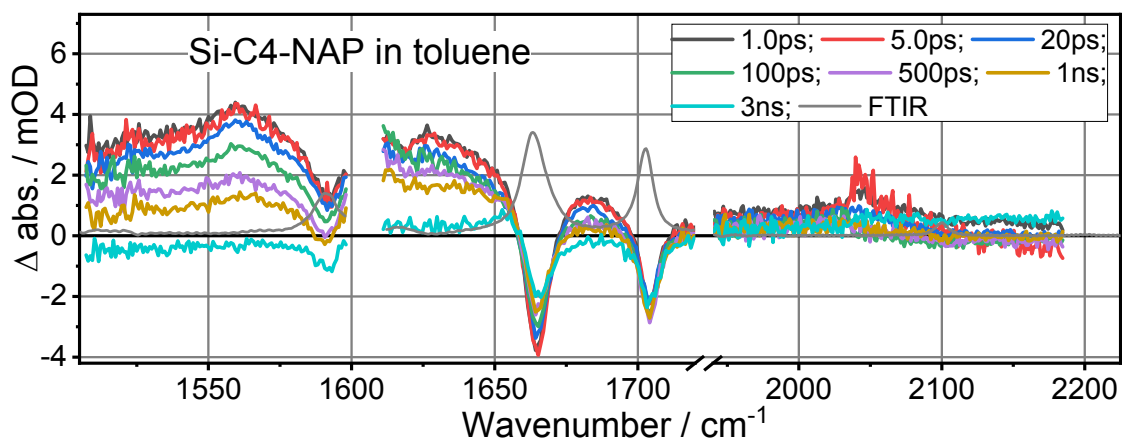


Fig. S4. Transient spectra in mid-IR region for Si-C4-NAP in toluene excited by 400 nm pulses.

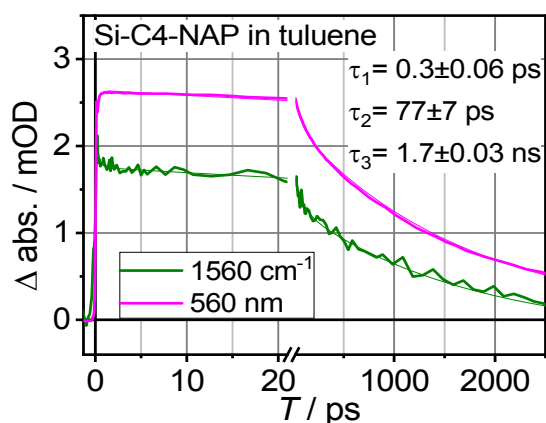


Fig. S5. Transient kinetics for Si-C4-NAP in toluene at indicated frequencies (thick lines, 560 nm line was normalized by 0.03 to match the intensities) and their fits with three-exponential functions (thin lines of matching colors). The fit parameters are shown as inset.

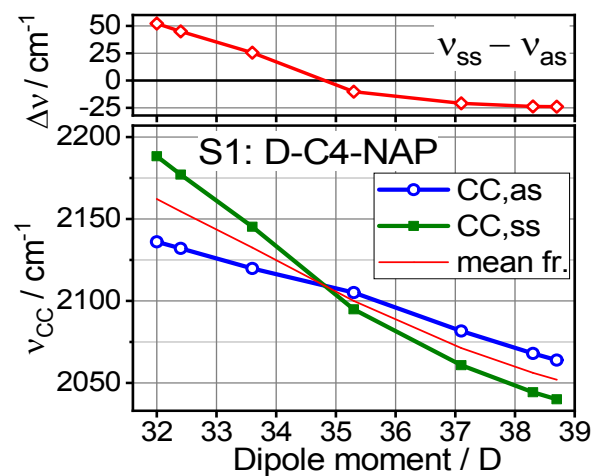


Fig. S6. (top) The frequency difference between $\nu_{CC,ss}$ and $\nu_{CC,as}$ as a function of the dipole moment of the D-C4-NAP compound in S₁ state, DFT computed in DCM. (bottom) A correlation of the $\nu_{CC,ss}$ and $\nu_{CC,as}$ mode frequencies with the dipole moment of the compound.

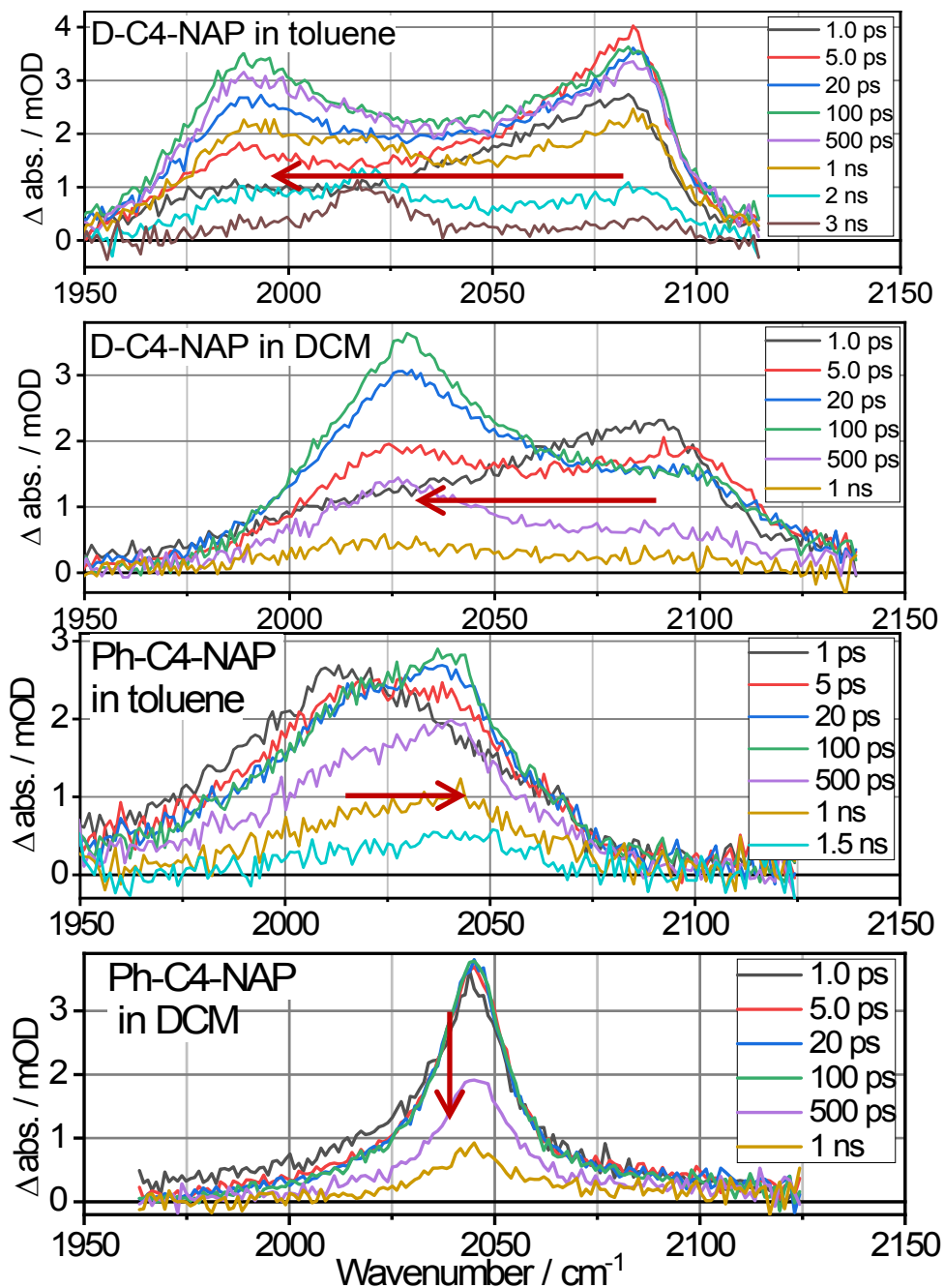


Fig. S7. Transient absorption spectra for the four systems in the C≡C region.

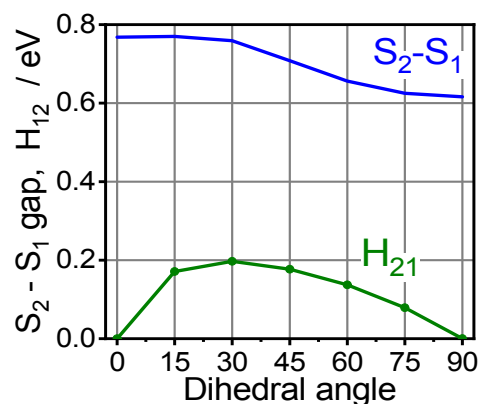


Fig. S8. Computed S_2-S_1 energy gap and the H_{DA} (H_{12}) coupling dependences on torsional angle θ .

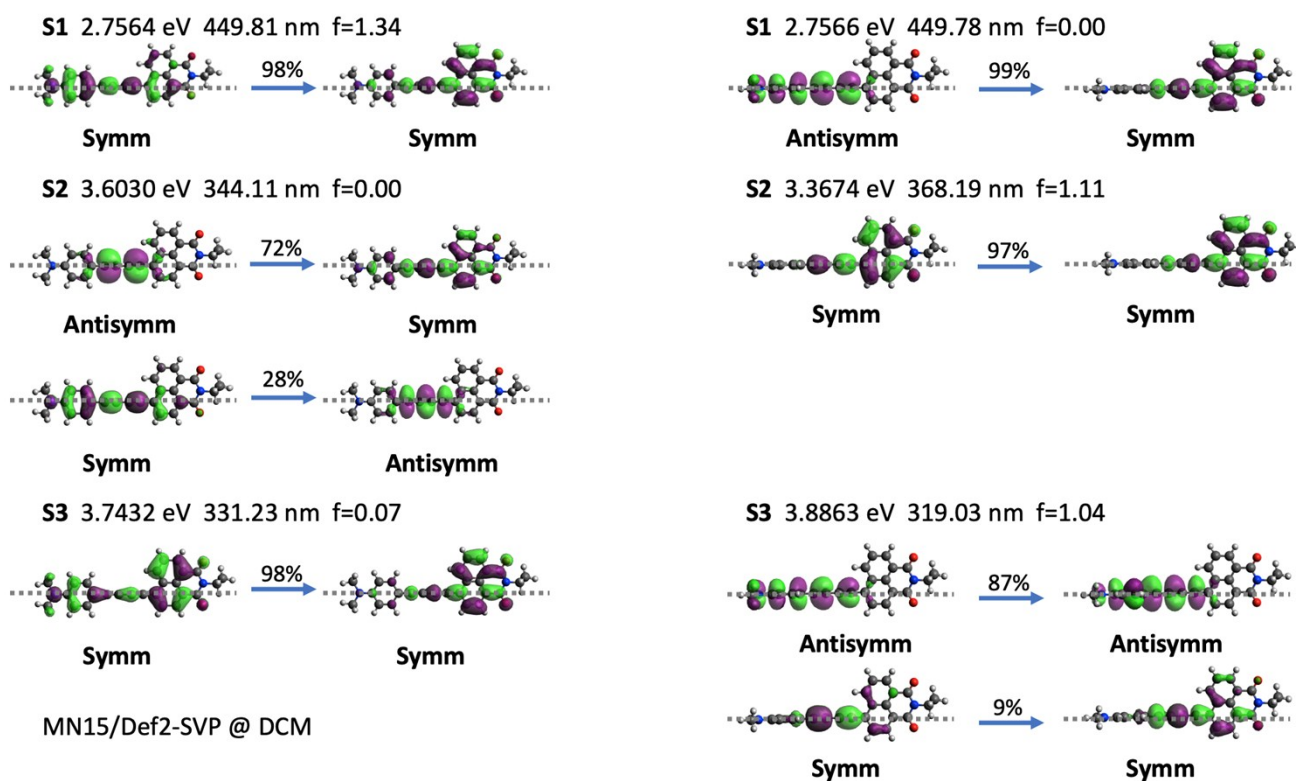
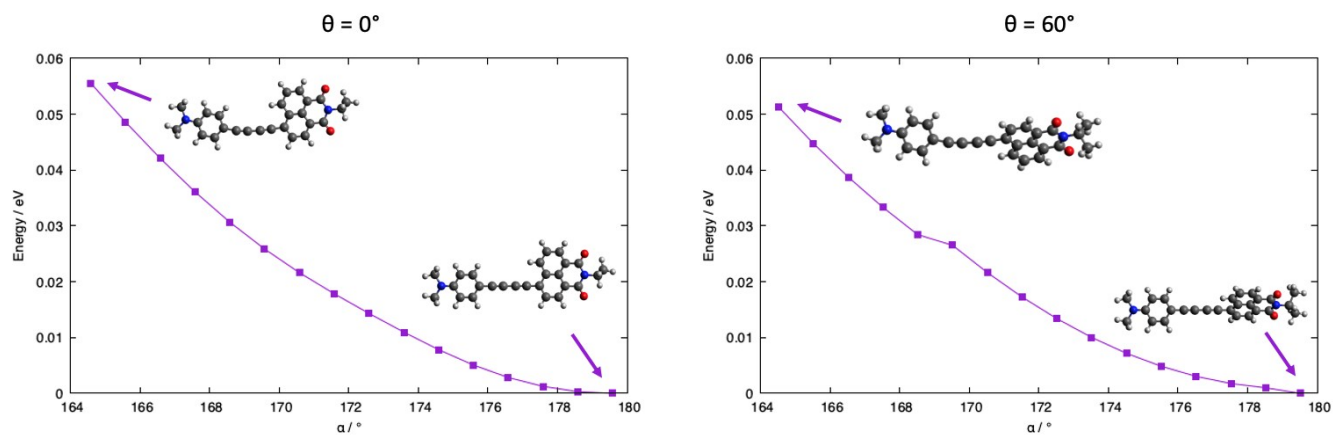
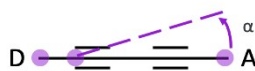


Fig. S9. Leading natural transition orbitals for $S_0 \rightarrow S_1$ and $S_0 \rightarrow S_2$ transitions of D-C4-NAP with their contributions in % above the arrow. The transition energy (in eV), transition wavelength, and the oscillator strength (f) values are shown. The symmetry of the orbitals with respect to the plane shown with dots is indicated.

MN15/Def2-SVP
@ DCM



State	$\alpha = 165^\circ$		$\alpha = 180^\circ$	
	Energy / eV	f	Energy / eV	f
S1	2.75	1.27	2.76	1.34
S2	3.59	0.00	3.60	0.00
S3	3.74	0.09	3.74	0.07
S4	3.85	0.00	3.88	0.00

State	$\alpha = 165^\circ$		$\alpha = 180^\circ$	
	Energy / eV	f	Energy / eV	f
S1	2.75	0.47	2.76	0.39
S2	3.41	0.76	3.40	0.83
S3	3.81	0.38	3.84	0.49
S4	3.96	0.24	3.97	0.23

Fig. S10. (top) Ground state energies as a function of the bend angle α at two torsion angles θ of 0° (left) and 60° (right) for D-C4-NAP in DCM. (bottom) The energies and oscillator strengths for $S_1 - S_4$ singlet excited states for two bend angles: $\alpha = 165^\circ$ and $\alpha = 180^\circ$.

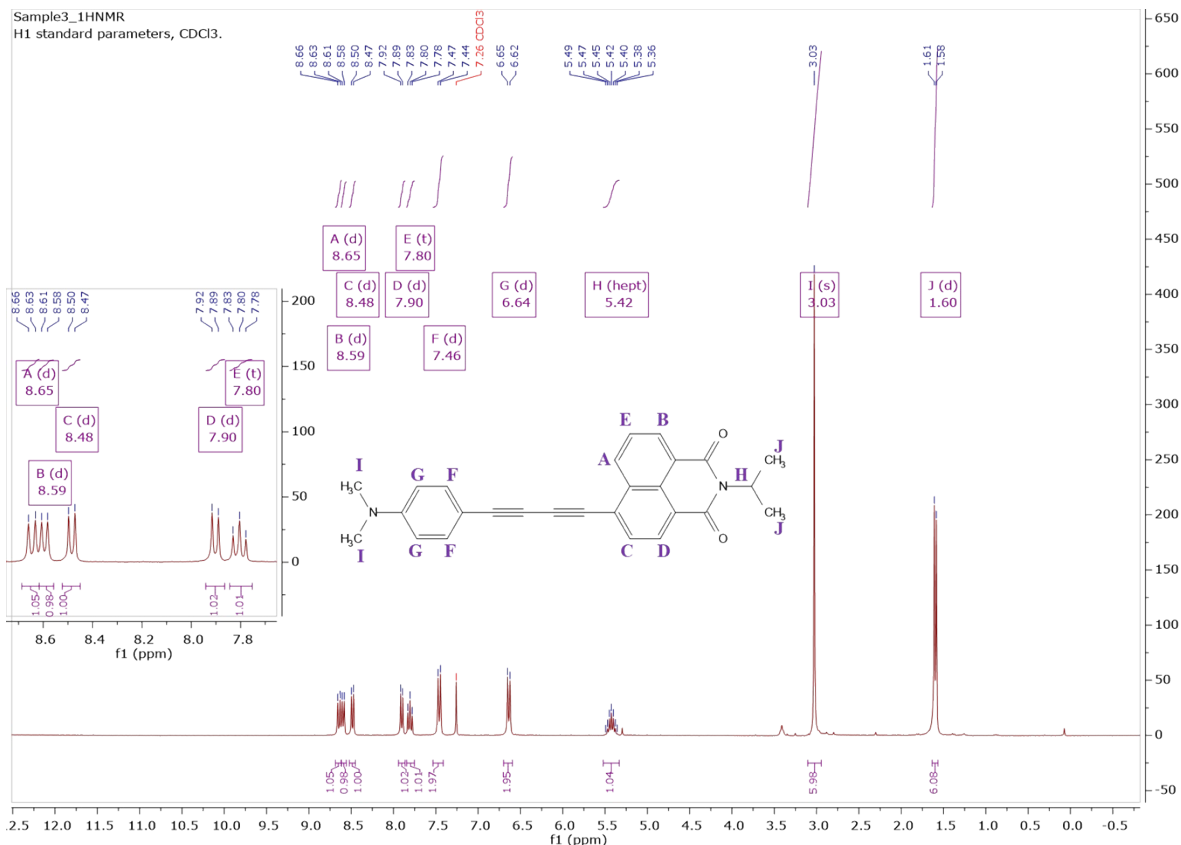


Fig. S11. ¹H NMR Spectra of D-C₄-NAPiPr

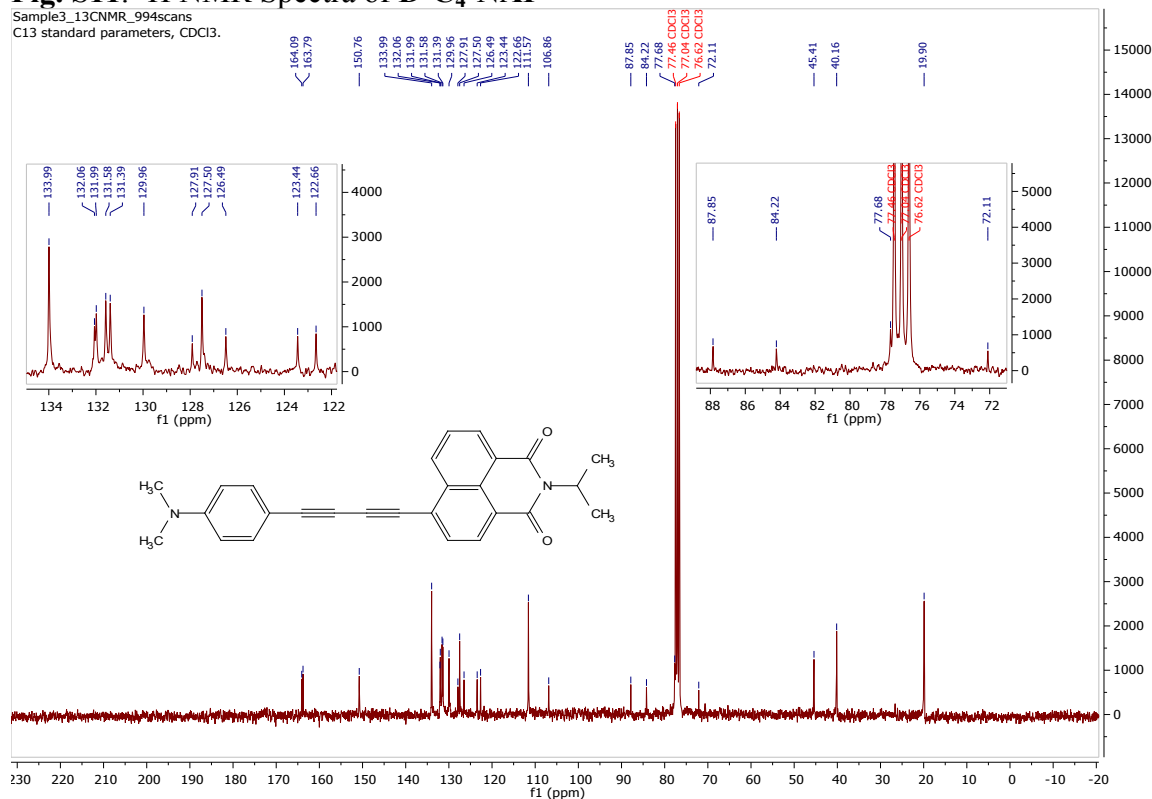


Fig. S12. ¹³C NMR Spectra of D-C₄-NAPiPr

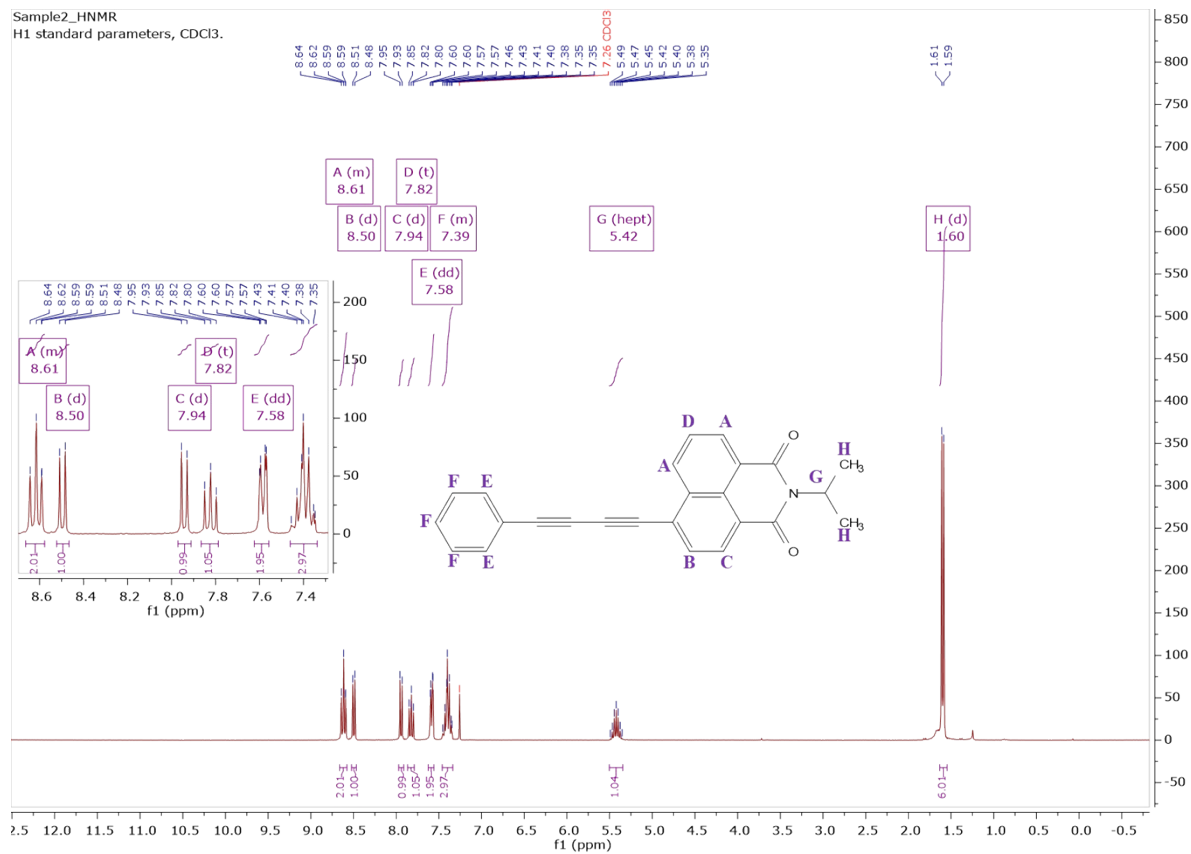


Fig. S13. ¹H NMR Spectra of Ph-C₄-NAPiPr

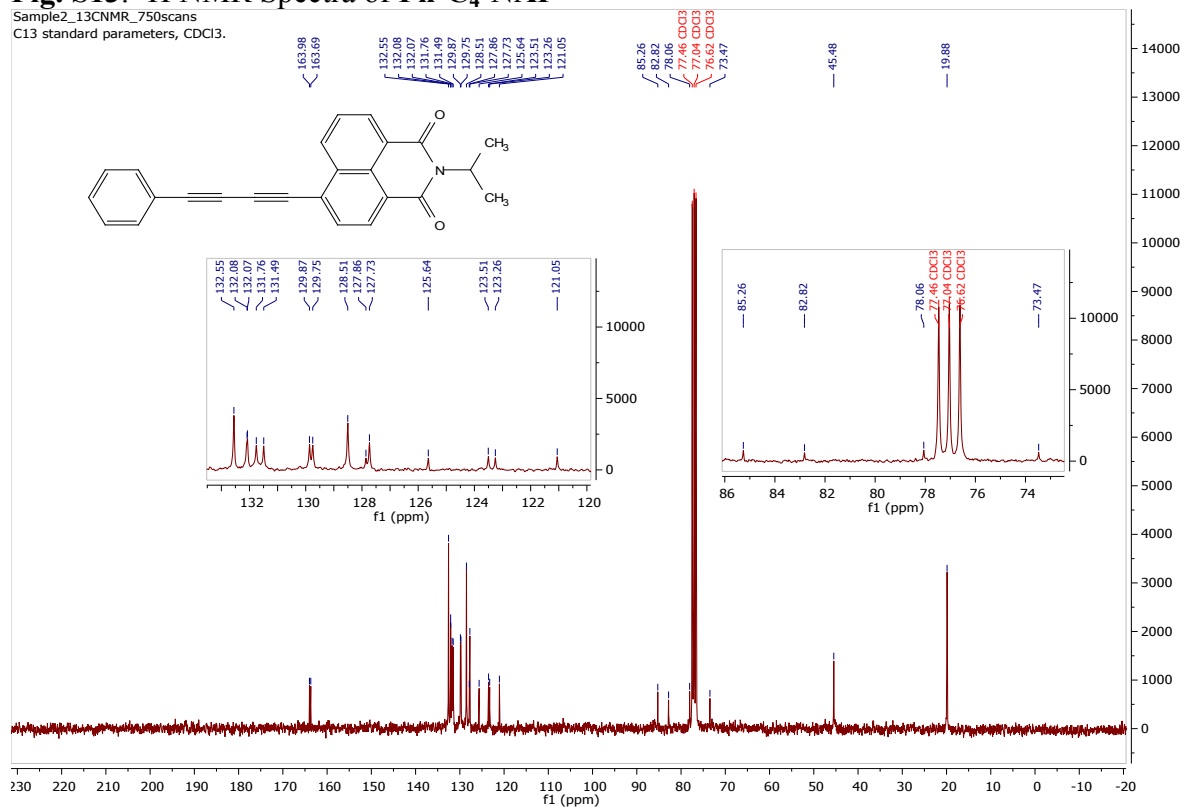


Fig. S14. ¹³C NMR Spectra of Ph-C₄-NAPiPr

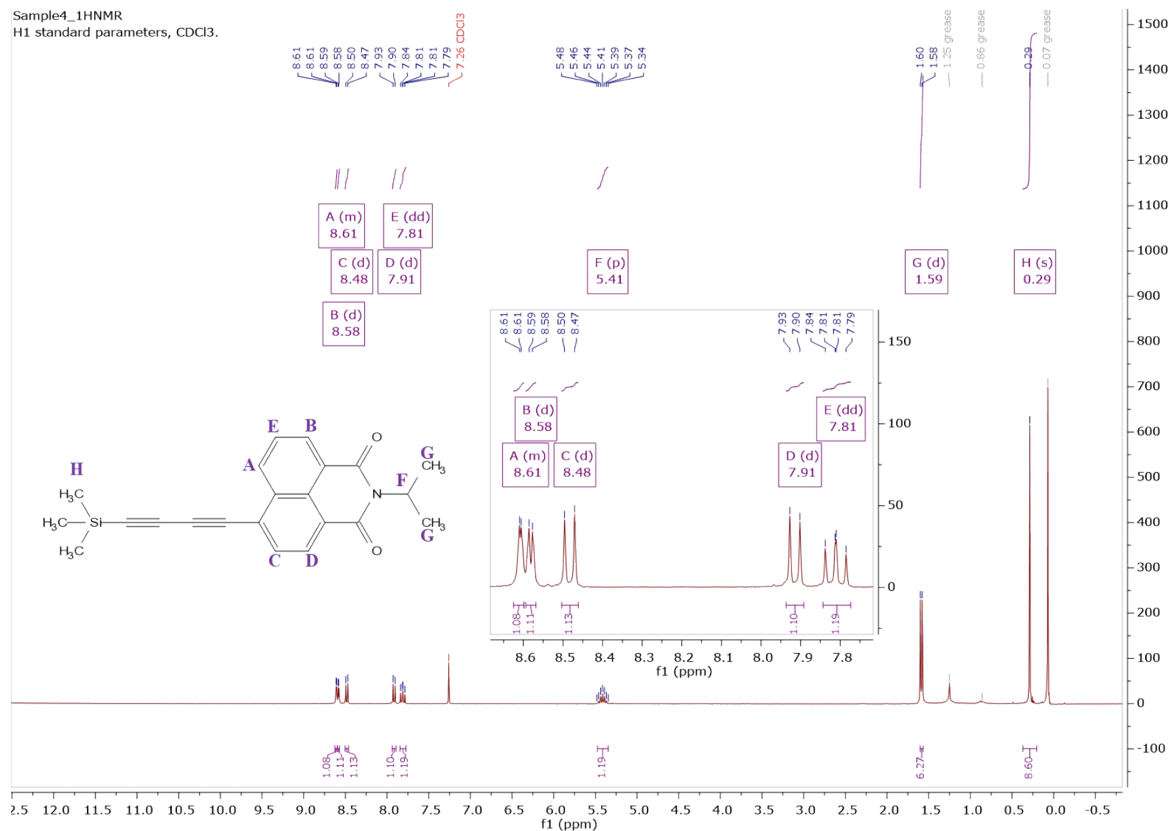


Fig. S15. ¹H NMR Spectra of TMS-C₄-NAPiPr

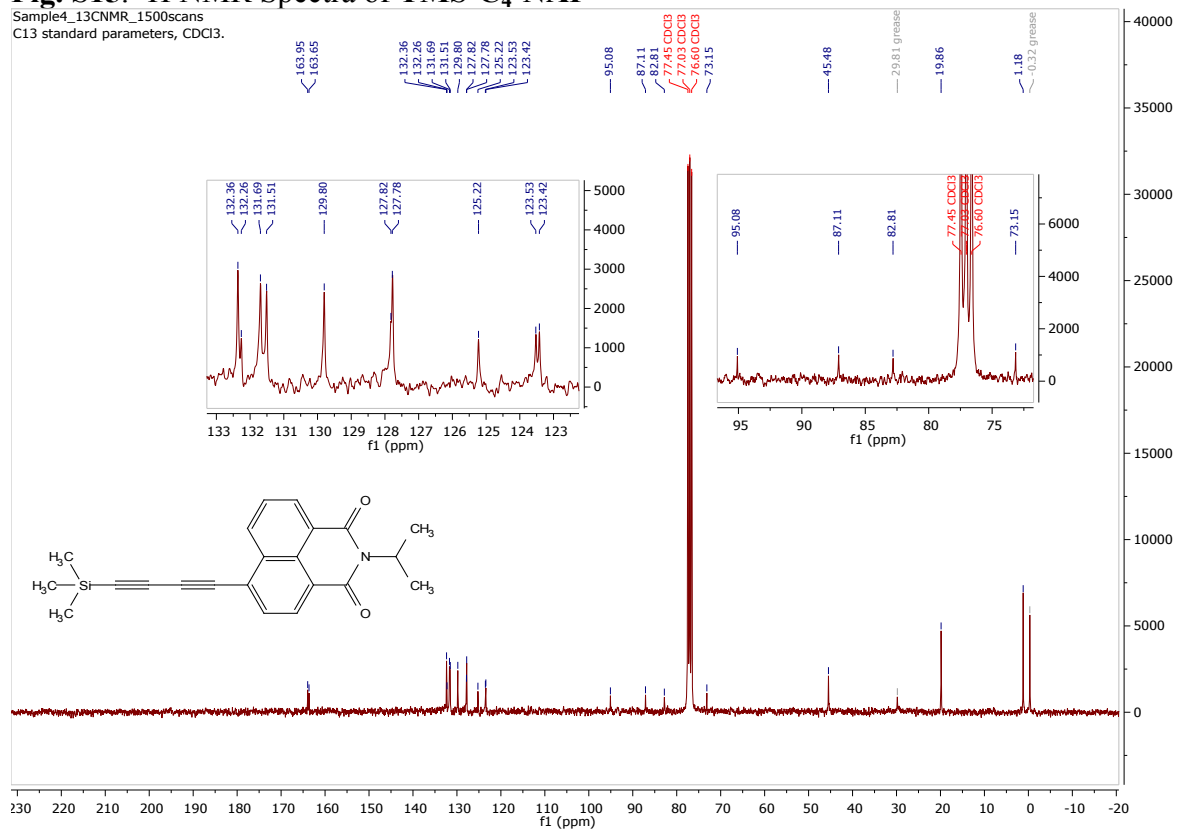


Fig. S16. ¹³C NMR Spectra of TMS-C₄-NAPiPr

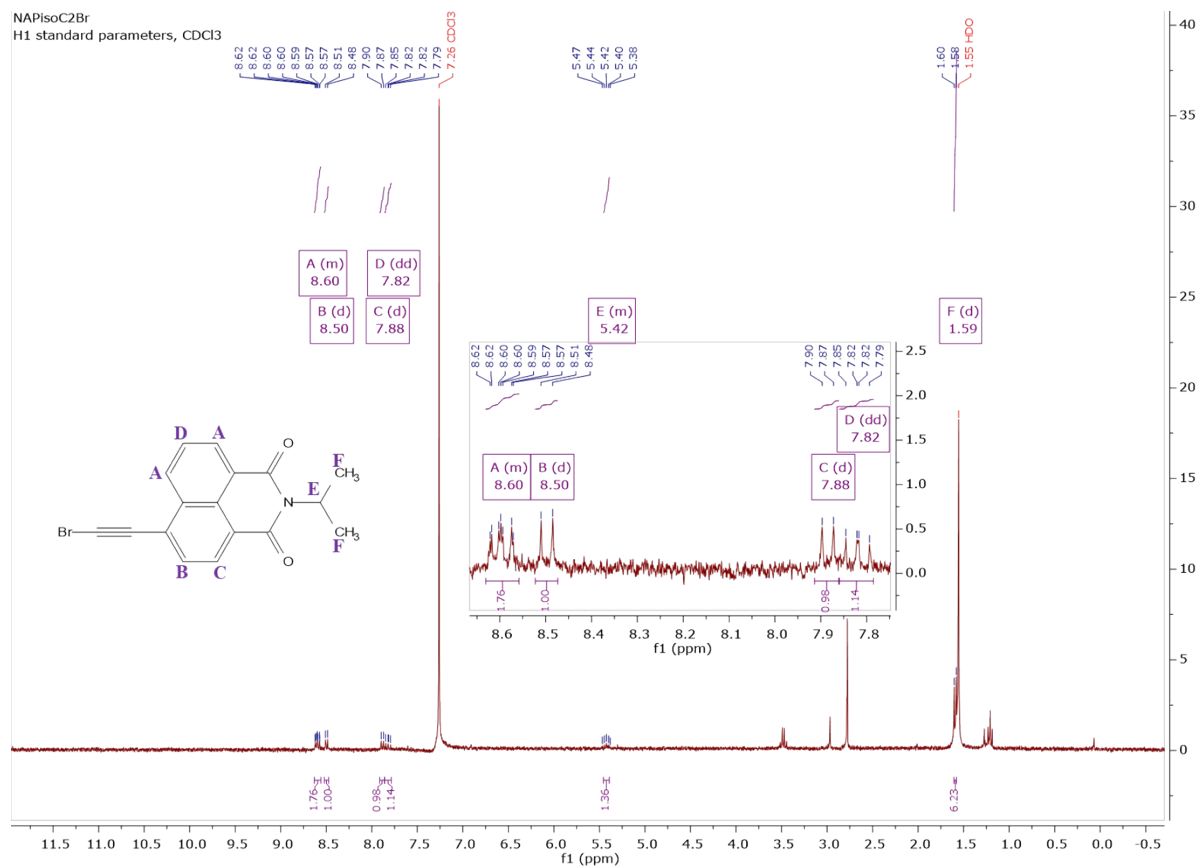


Fig. S17. ¹H NMR Spectra of Br-C₂-NAPiPr

1. Susannah D. Banziger, Eileen C. Judkins, M. Z. and T. R. Diruthenium-DMBA Bis-Alkynyl Compounds with Hetero- and Extended- Aryl Appendant. *Chinese J. Inorg. Chem.* **33**, 2103–2109 (2017).